

Human Pluripotent Stem Cell-Derived Radial Glia Recapitulate Developmental Events and Provide Real-Time Access to Cortical Neurons and Astrocytes

LISHU DUAN, CHIAN-YU PENG, LIULIU PAN, JOHN A. KESSLER

Key Words. Radial glia • Human embryonic stem cells • Human iPS cells • Cortical neuron • Astrocytes • Cortical interneuron

Department of Neurology,
Northwestern University
Feinberg School of Medicine,
Chicago, Illinois, USA

Correspondence: Lishu Duan, Ph.D.,
Department of Neurology,
Northwestern University
Feinberg School of Medicine, 303
East Chicago Avenue, Chicago,
Illinois 60611-3008, USA.
Telephone: 312-503-3583;
E-Mail: lishuduan2011@u.
northwestern.edu

Received July 10, 2014; accepted
for publication January 19, 2015;
published Online First on April 1,
2015.

©AlphaMed Press
1066-5099/2015/\$20.00/0

[http://dx.doi.org/
10.5966/sctm.2014-0137](http://dx.doi.org/10.5966/sctm.2014-0137)

ABSTRACT

Studies of human cerebral cortex development are limited by difficulties in accessing and manipulating human neural tissue at specific development stages. We have derived human radial glia (hRG), which are responsible for most cerebral cortex neurogenesis, from human pluripotent stem cells. These hRG display the hallmark morphological, cellular, and molecular features of radial glia in vitro. They can be passaged and generate layer-specific subtypes of cortical neurons in a temporal and passage-dependent fashion. In later passages, they adopt a distinct progenitor phenotype that gives rise to cortical astrocytes and GABAergic interneurons. These hRG are also capable of following developmental cues to engraft, differentiate, migrate, and integrate into the embryonic mouse cortex when injected into E14 lateral ventricles. Moreover, hRG-derived cells can be cryopreserved at specific stages and retain their stage-specific phenotypes and competence when revived. Our study demonstrates that cultured hRG maintain a cell-intrinsic clock that regulates the progressive generation of stage-specific neuronal and glial subtypes. It also describes an easily accessible cell source for studying hRG lineage specification and progression and an on-demand supply of specific cortical neuron subtypes and astrocytes. *STEM CELLS TRANSLATIONAL MEDICINE* 2015;4:437–447

SIGNIFICANCE

This study describes a protocol that uses human pluripotent stem cells to differentiate into radial glia and, in turn, generate a large number of cortical pyramidal neurons, interneurons, and astrocytes that are important for both mechanistic studies and use in cellular replacement therapy.

INTRODUCTION

The cerebral cortex, the most complex structure in the mammalian brain, originates from a single layer of symmetrically dividing neuroepithelial (NE) cells that can be characterized by their pseudostriated morphology and a combination of molecular markers, including nestin, Sox2, and vimentin [1]. As these early neural progenitors divide and begin to expand the cortical plate, they acquire an elongated bipolar morphology and are termed radial glia (RG). Markers that distinguish RG from NE cells in humans include brain lipid-binding protein (BLBP) and glial fibrillary acidic protein (GFAP) [2–4]. RG reside in the ventricular zone (VZ) and follow a cell-intrinsic mechanism to sequentially generate cortical neurons in the six-layered neocortex, with the deep layer neurons (layers V–VI) first and the superficial layers (layers II–IV) next [5, 6]. This is accomplished through expansion of RG-derived intermediate progenitor cells located in the embryonic subventricular

zone (SVZ). The human embryonic SVZ is subdivided into an inner SVZ and a wider outer SVZ, which is believed to account for the greatly expanded cortical structure [7]. At the end of neurogenesis, RG switch from being neurogenic to gliogenic as they detach from the ventricular surface and acquire multipolar morphology and additional astrocytic characteristics. Cortical astrogliogenesis continues into the postnatal period, during which time SVZ RG also begin generating GABAergic interneurons [8, 9].

Our knowledge of the origin and lineage progression of human RG has largely been extrapolated from rodent studies owing to the limited access to human tissue. Recent live imaging of organotypic culture of fetal human ventricular radial glia has provided anatomical and cellular insights into radial glial properties *ex vivo* [10]. Human pluripotent stem cells (hPSCs), including human embryonic stem cells (hESCs) and induced pluripotent stem cells (iPSCs), provide valuable tools for studying human neural development,

modeling central nervous diseases, and providing potential cell replacement therapies. Directed differentiation of hPSCs toward the neuroectodermal lineage produces neural rosettes, structures that resemble the neural tube with organized polarized columnar NE cells [11]. Bipolar cells with radial fibers extending from rosette structures have been documented; however, a thorough expression analysis of hRG-specific molecular markers and the ability to generate temporally distinct populations of cortical neurons and astrocytes have not been demonstrated [12–14]. Several studies have shown that generation of cortical neurons from hPSCs mirrors the temporal sequence *in vivo*, but the isolation of temporally restricted hRG populations that generate selected neuronal subtypes has not been reported. It has also been unclear whether cultured hRG undergo the developmental transition from being neurogenic to astroglial, similar to the transition *in vivo* [15–17].

In the present study, we generated a distinct population of cells from human H7 ESCs and two iPSCs lines that display the morphological and molecular characteristics of hRG. These cultured hRG followed a cell-intrinsic mechanism to first sequentially generate cortical neurons of different layers and then transition into a late progenitor that gave rise to astrocytes and interneurons. When transplanted into embryonic mouse lateral ventricle, these hRG followed developmental cues and migrated to the appropriate cortical layer as radially oriented pyramidal neurons. Moreover, stage-specific hRG cultures could be frozen and stably maintained the stage-specific RG phenotype after thawing, thus providing an easily accessible source for studying hRG lineage specification and a real-time supply of specific cortical neurons and astrocytes.

MATERIALS AND METHODS

hPSC Culture

The H7 hESC line and iPSCs were maintained on irradiated mouse embryonic fibroblasts in hESC medium containing Dulbecco's modified Eagle's medium (DMEM)/F12, 20% knockout serum replacement, 0.1 mM nonessential amino acids, 2 mM L-glutamine, 100 μ M β -mercaptoethanol, and 10 ng/ml basic fibroblast growth factor (bFGF). Two iPSC lines were derived from normal human dermal fibroblasts via retroviral reprogramming with a polycistronic vector containing Oct4, Sox2, Klf4, and c-Myc. These iPSCs cell lines had been characterized previously for pluripotency [18].

Differentiation of hPSCs

hPSCs were harvested as clumps with 1 mg/ml collagenase onto low-adherence flasks in hESC medium without bFGF to allow differentiation. Three days later, the medium was switched to N2 containing neurosphere medium (DMEM/F12, 0.1 mM nonessential amino acids, 1 \times N2 supplement, 100 μ M β -mercaptoethanol, and 8 μ g/ml heparin) with 20 ng/ml bFGF and 20 ng/ml epidermal growth factor (EGF) for 5 days. At day 8, homogenous neurospheres were confirmed under a dissection microscope, hand-picked, and dissociated into single cells with Accutase (Life Technologies, Carlsbad, CA, <http://www.lifetechnologies.com>). Next, 1.5 \times 10⁵ cells were plated onto poly-D-lysine-coated 24-well plates in differentiation medium with B27 and 0.4 ng/ml EGF. The medium was refreshed every 5 days. The cells were harvested 32 days later with Accutase and split at a density of 1 \times 10⁵ cells per 24-well plate well. The cells were maintained

in the differentiation medium until confluence, when they were passaged. For astrocyte differentiation at later passages (beyond passage 5), the cells were cultured in serum containing medium (DMEM, 10% fetal bovine serum, and 0.1 mM nonessential amino acids) for 7 days.

5'Ethynyl-2'Deoxyuridine Labeling and Detection

Click-iT EdU Imaging Kits (catalog no. C10339; Life Technologies) were used to label cells with 5' ethynyl-2' deoxyuridine (EdU) and for detection. EdU was added to the culture medium at a final concentration of 10 μ M and incubated with the cells for 2 hours. The cells were then fixed with 4% paraformaldehyde (PFA) for 15 minutes and washed twice with 1 \times phosphate-buffered saline (PBS). Primary antibodies in 1 \times PBS, 1% bovine serum albumin (BSA), 0.25% Triton X-100, and 10% donkey serum were applied overnight at 4°C. After 3 PBS washes, secondary antibodies were added for 1 hour at room temperature, followed by 2 PBS washes. The EdU reaction cocktail was added for 30 minutes at room temperature. The cells were then washed twice with PBS and incubated with 4',6-diamidino-2-phenylindole (DAPI) for nuclear staining for 15 minutes. Three PBS washes were performed before the coverslips were mounted for microscopic analysis.

Immunocytochemistry, Immunohistochemistry, and Imaging

The cells were fixed in 4% PFA for 15 minutes, followed by two 1 \times PBS washes. P3 brains were dissected out and immediately fixed with 4% PFA for 2 hours, followed by incubation with 30% sucrose in 1 \times PBS overnight. Coronal slices of brains in Tissue-Tek O.C.T. (Sakura Finetek, Alphen aan den Rijn, The Netherlands, <http://www.sakura.com>) blocks were prepared as 16- μ m slices with a cryostat. The cells and tissue sections were incubated with primary antibodies in staining buffer (1 \times PBS, 1% BSA, and 0.25% Triton X-100) with 10% donkey serum as a blocking agent. A list of the primary antibodies is provided in supplemental online Figure 5. After 3 PBS washes, fluorophore-conjugated Alexa Fluor goat secondary antibodies (1:1,000) (Life Technologies) were incubated with the cells and tissue sections in staining buffer with DAPI nuclear staining for 1 hour. After three washes, the slides were mounted in ProLong Gold antifade reagent (Life Technologies). Images were taken on a Zeiss Axiovert epifluorescence microscope (Carl Zeiss, Jena, Germany, <http://www.zeiss.com>) and a Leica DM6000 confocal microscope (Leica, Heerbrugg, Switzerland, <http://www.leica.com>). The cells were counted manually using NIH ImageJ software. For *in vitro* counting, the total cell number was identified based on DAPI staining, and the subtypes of cells were identified and counted based on relevant marker staining. For *in vivo* counting, transplanted cells were identified by green fluorescent protein (GFP) antibody detection, and this served as the total cells. The subtypes of cells within this population were identified and counted based on relevant marker staining.

In Utero Intraventricular Cell Transplantation

All animal procedures were performed in accordance with the Public Service Policy on Human Care and Use of Laboratory Animals, and the Northwestern University Institutional Animal Care and Use Committee approved all the procedures. The cells were labeled with an enhanced GFP lentivirus, harvested after 72 hours, and resuspended in culture medium at a density of 10,000 cells per microliter. Pregnant CD1 mice (Charles River Laboratories,

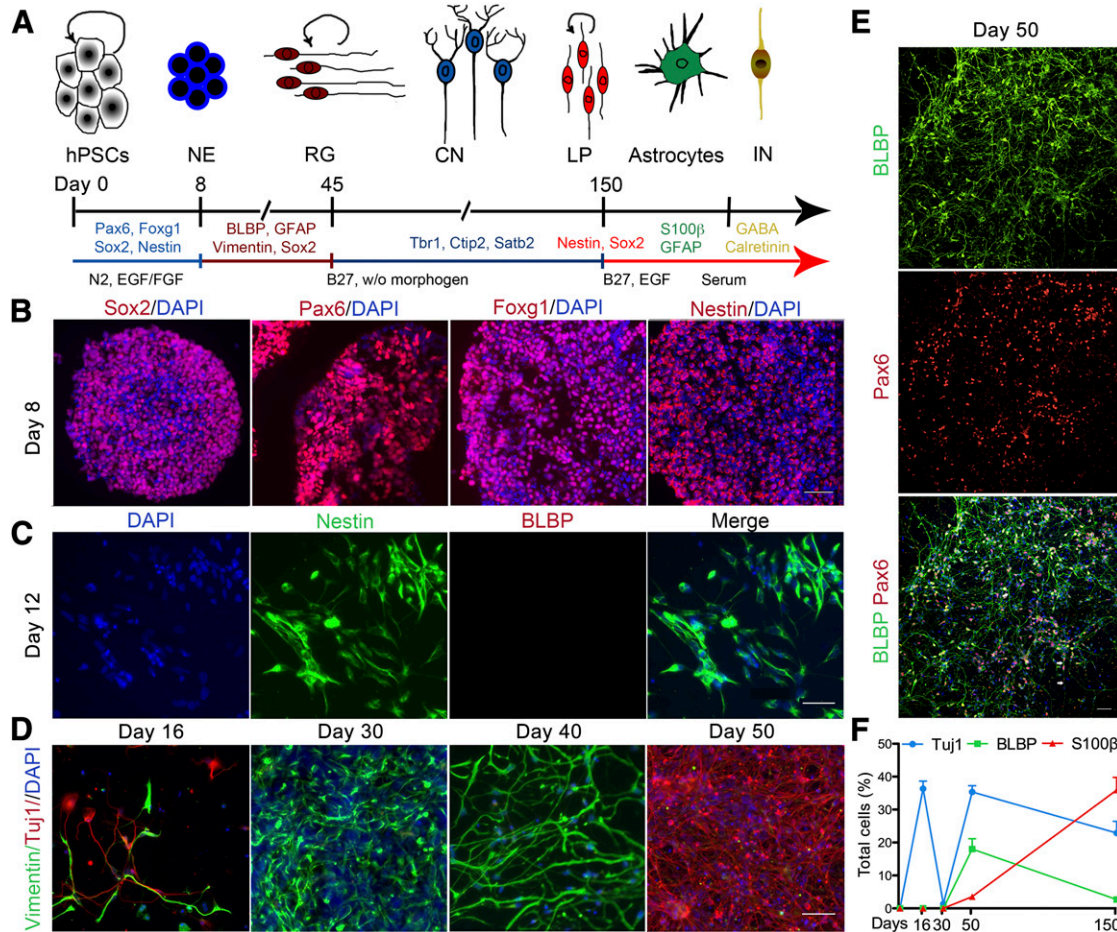


Figure 1. Differentiation of RG from hESCs. **(A):** Summary of the different stages of cells in culture. hESCs were first differentiated to NE cells, followed by differentiation into RG cells without morphogens. RG continuously generated CNs until around day 150, when the RG transitioned to a LP stage that primarily generated astrocytes and some INs. **(B):** At day 8, early neural progenitors expressed neuroepithelial markers Sox2, Pax6, Foxg1, and nestin. Nuclei are indicated by DAPI staining. **(C):** Day 12 cells expressed the neuroepithelial marker nestin but were negative for the RG marker BLBP. **(D):** A brief wave of Tuj1-positive neurons was present before the appearance of RG and then reappeared after the generation of RG. Neural progenitors were stained with vimentin. **(E):** Day 50 cultures consisted of long process-bearing cells, which stained positive for BLBP and for Pax6 in the nucleus. RG typically exhibited two types of morphology, unipolar (top white arrow) or bipolar (bottom two white arrows). **(F):** Temporal expression of lineage markers among total cells. Data are mean ± SEM; n = 5. Scale bars = 50 μm. Abbreviations: BLBP, brain lipid-binding protein; CNs, cortical neurons; DAPI, 4',6-diamidino-2-phenylindole; EGF, epidermal growth factor; FGF, fibroblast growth factor; GFAP, glial fibrillary acidic protein; hESCs, human embryonic stem cells; INs, interneurons; LP, late progenitor; NE, neural epithelial; RG, radial glia; w/o, without.

Wilmington, MA, <http://www.criver.com>) with embryos at gestational stage E14 were anesthetized with inhalation of 2.5% isoflurane anesthetic in 100% oxygen administered using a VetEquip rodent anesthesia machine (VetEquip Inc., Pleasanton, CA, <http://www.vetequip.com>). The abdomen was shaved and wiped with 80% alcohol, and a 2-cm midline laparotomy was performed. One uterine horn at a time was taken out carefully, and the embryos were constantly moisturized with saline. The embryos were positioned to reveal the brain, and only one side of each brain was injected with 1 μl of the cell suspension into the lateral ventricle region with a finely drawn glass micropipette. After injection, the uterine horns were returned into the abdomen, antibiotic Baytril (Bayer Animal Health, Monheim, Germany, <http://www.animalhealth.bayer.com>) at a dose of 5 mg/kg was administered, and the mother was sutured. After the mother had recovered from the surgery, 0.5 mg/kg analgesic buprenorphine was injected subcutaneously.

Statistical Analysis

Student’s t test, assuming unequal variance, was performed for experiments with only two conditions. One-way analysis of variance (ANOVA), followed by Bonferroni’s post hoc test, was used to determine the statistical significance for multiple group comparisons. All data are presented as the mean ± SEM.

RESULTS

Differentiation to Radial Glia Follows Developmental Principles

To generate radial glia, we first allowed hESCs to spontaneously differentiate into NE cells using serum-free suspension culture for 3 days [19], followed by 5 days of expansion in the presence of bFGF and EGF. The differentiation timeline, added factors, and relevant phenotype are shown in Figure 1A. Highly compact

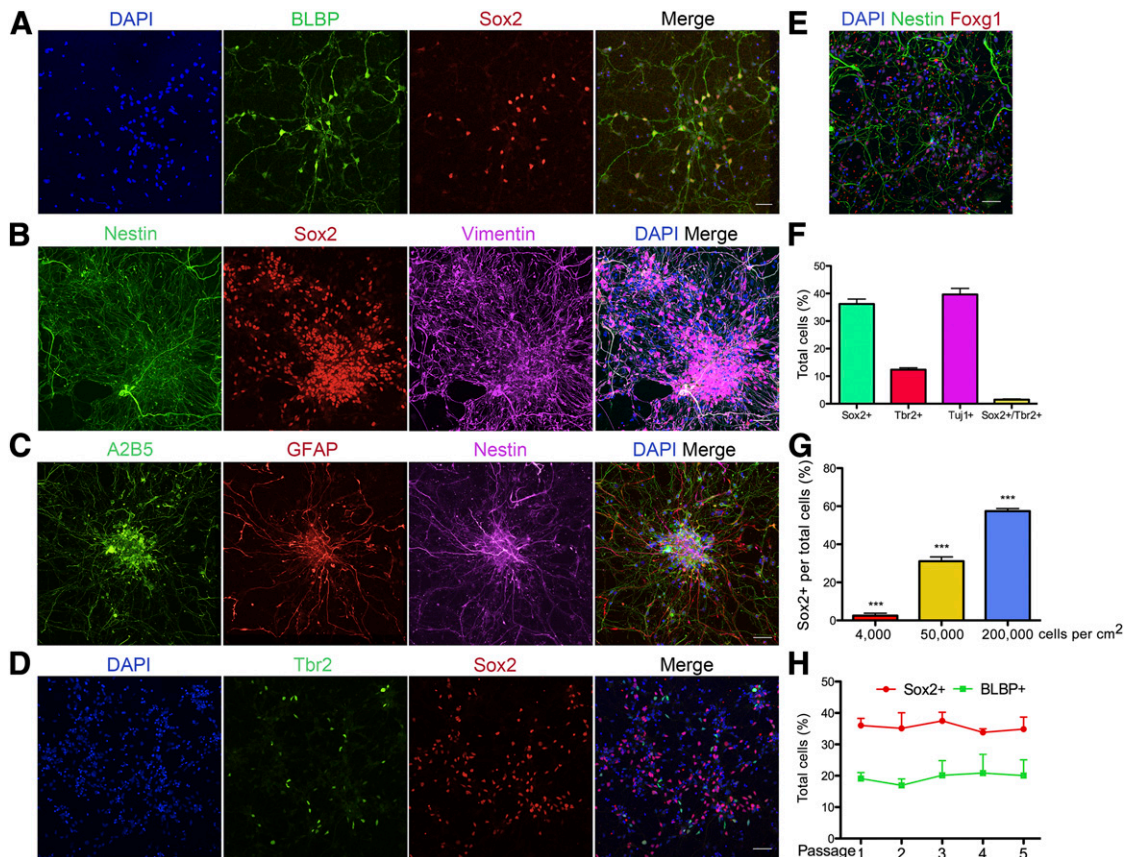


Figure 2. Characteristics of radial glia culture derived from human embryonic stem cells (hESCs). **(A–E):** Molecular marker characterization of hESC-derived radial glia (RG) cells. **(A):** BLBP-positive cells also stained for Sox2. **(B):** RG coexpressed nestin, vimentin, and Sox2. **(C):** Nestin-positive RG also expressed A2B5 and GFAP. **(D):** Tbr2-positive intermediate neuronal progenitor cells are also present in the RG cultures. Tbr2 and Sox2 rarely colocalize. **(E):** Nestin-positive RG retained expression of forebrain neural stem cell marker Foxg1. **(F):** Quantification of cell type-specific markers among total cells in RG cultures. Sox2 = 36.2% ± 1.8%; Tbr2 = 12.6% ± 0.7%; Tuj1 = 39.6% ± 2.2%; Sox2 and Tbr2 copositive = 1.5% ± 0.2%; *n* = 9. **(G):** Percentages of Sox2-positive progenitors among total cells varied according to plating density. Low density = 2.5% ± 1.3%; normal density = 31.1% ± 2.3%; high density = 57.4% ± 1.3%. One-way analysis of variance, $F(2, 4) = 269.8$; $p < .0001$. **(H):** RG were passaged five times and monitored for maintenance of RG markers. The percentages of both Sox2- and BLBP-positive cells remained constant during the first five passages. Scale bars = 50 μ m. Data are presented as mean ± SEM. ***, $p < .0001$. Abbreviations: BLBP, brain lipid-binding protein; DAPI, 4',6-diamidino-2-phenylindole; GFAP, glial fibrillary acidic protein.

and translucent neurospheres were then selected for subsequent study (supplemental online Fig. 1A). These neurospheres expressed a battery of forebrain NE markers, including Sox2, Pax6, Foxg1, and nestin (Fig. 1B). The neurospheres were then dissociated, plated as single cells, and allowed to differentiate without growth factors. At day 12, the plated cells still expressed the NE marker nestin but not the hRG marker brain lipid-binding protein (BLBP) (Fig. 1C). At around day 16, we began to observe an early, transient wave of Tuj1-positive, Vglut1-positive neurons (Fig. 1D, 1F; supplemental online Fig. 1C). These early neurons expressed reelin (supplemental online Fig. 1B), suggesting that they might be Cajal-Retzius neurons, which play a key role in the formation of the cerebral cortex [20].

Radial-shaped vimentin-positive cells first appeared at around day 16 and steadily increased in number through day 40 (Fig. 1D). When passaged at day 40, these cultures were able to generate significant numbers of neurons while maintaining a progenitor population with radial morphology (Fig. 1D). These long radial-shaped cells expressed the characteristic hRG molecular marker BLBP and Pax6, a key factor in the specification of neurogenic RG (Fig. 1E) [21, 22]. The same protocol applied to iPSCs

similarly generated hRG (supplemental online Fig. 2). However, we mainly present the differentiation results from hESC-generated hRGs in the following sections.

Cellular and Molecular Characterization of hESC-Derived Radial Glia

In the absence of the lateral ventricle as a structural landmark, the identification of RG *in vitro* relies on a thorough analysis of the molecular markers, morphology, and functional properties. BLBP-positive RG also expressed the neural stem cell (NSC) marker Sox2 (Fig. 2A). Furthermore, both nestin and vimentin costained the long radial fibers of the cells that expressed nuclear Sox2 (Fig. 2B). The cells also expressed Foxg1 (Fig. 2E), a transcription factor essential for progenitor cell proliferation and differentiation in the telencephalon [23, 24], but not the hindbrain marker Hoxb4 (data not shown). Finally, the hESCs-derived RG expressed GFAP, A2B5, and nestin (Fig. 2C). The detailed staining pattern of BLBP, Nestin, and GFAP is also shown in higher resolution (supplemental online Fig. 4). Tbr2-expressing cells [25] were present in our cultures, but they rarely coexpressed Sox2, suggesting

that they are more committed transient-amplifying secondary progenitors (Fig. 2D). Sox2-positive progenitors accounted for $36.2\% \pm 1.8\%$ of the total cells, Tuj1-positive neurons for $39.6\% \pm 2.2\%$, and Tbr2-positive progenitors for $12.6\% \pm 0.7\%$ ($n = 9$). The remaining 10% of the cells were uncharacterized.

Next, we wondered whether we could enrich the percentage of RGs in culture. Previous studies suggested that plating at a high density for the initial passage is critical for cortical neuron specification from hPSCs [26]. We plated dissociated neurospheres at different cell densities and monitored RG formation at the end of 40 days. Although numerous GFAP-positive RG were present in the high-density groups, in the low-density groups, the number was essentially none (supplemental online Fig. 3A). Based on the larger size of the nucleus and the lack of staining for the NSC markers nestin and Sox2, the cells in the low-density groups might be non-neural (data not shown).

High-density plating increases the cell-cell contact, which enhances the Notch signaling essential for specification and maintenance of RG [27–29]. Western blot analysis confirmed that low-density cultures had significantly less Notch signaling than did high-density cultures (supplemental online Fig. 3C). To determine whether Notch signaling played a role in RG formation in our differentiation culture, iPSC- or hESC-derived neurospheres were each plated in the presence or absence of $1 \mu\text{M}$ γ -secretase inhibitor DAPT (*N*-[*N*-(3,5-difluorophenacetyl)-*L*-alanyl]-*S*-phenylglycine *t*-butyl ester). In both cases, DAPT treatment led to failure of RG differentiation (supplemental online Fig. 3B). We then asked whether varying the culture density and Notch signaling could enrich progenitors in already established RG cultures. Cultures plated at the standard density (5×10^4 cells per cm^2) had $31.1\% \pm 2.3\%$ Sox2-positive progenitors. High-density culture (2×10^5 cells per cm^2) significantly increased Sox2-positive cells to $57.4\% \pm 1.3\%$, and low-density culture (4×10^3 cells per cm^2) reduced the progenitor population dramatically down to $2.4\% \pm 1.3\%$ ($n = 4$, 1-way ANOVA, $p < .0001$; Fig. 2G). Cultures at normal density, 5×10^4 cells per cm^2 , were treated with dimethyl sulfoxide (DMSO), Notch ligands Delta-1 (200 $\mu\text{g}/\text{ml}$) or Jagged-1 (200 $\mu\text{g}/\text{ml}$), and γ -secretase inhibitor DAPT (1 μM) for 14 days and evaluated for culture composition. Compared with the DMSO group, the addition of Jagged-1 significantly increased the proportion of BLBP-positive RGs but Delta-1 had no effect. DAPT treatment showed a trend toward but not a significant reduction in the number of progenitor cells. The Tuj1-positive neuronal percentages were similar across all groups (supplemental online Fig. 3D).

hESC-Derived RG Generate Subtypes of Cortical Neurons in a Passage-Wise Manner

Passaging the hESC-derived RG cultures every 25 days for the first 5 months did not significantly alter the percentage of RG or Sox2+ NSCs in the culture (Fig. 2H). However, we then asked whether the developmental potential of the RG changed during this time by examining the phenotypes of the Tuj1-positive neurons generated by the RG. During corticogenesis, RG are responsible for generating glutamatergic pyramidal neurons in an inside-out fashion. At every passage, all neurons expressed Vglut1, a glutamatergic neuron marker (Fig. 3B), and no positive staining for the cortical interneuron marker glutamic acid decarboxylase 65/67, the cholinergic neuron marker cholinergic acetyl-transferase, or the dopaminergic neuron marker tyrosine hydroxylase was detected (data not shown). Early passage RG (passages 1–3) generated early-born neurons, as labeled by the deep layer markers Tbr1 (layer IV and V) and Ctip2 (layer V) (Fig. 3A, left and middle)

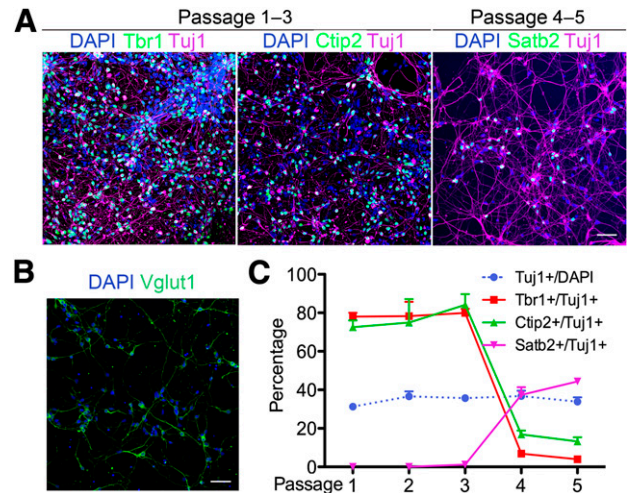


Figure 3. Human embryonic stem cell (hESC)-derived radial glia (RG) generate layer-specific cortical neurons sequentially in vitro. **(A):** Neurons in the early passage (1–3) cultures express deep layer markers Tbr1 (left) and Ctip2 (middle) but not Satb2; the superficial layer marker Satb2 first appeared after passage 3 (right). **(B):** Neurons in the RG cultures are positive for glutamatergic marker Vglut1. **(C):** Quantification and comparison of neuronal subtypes at different passages. Although the percentage of neurons (blue dotted line) remained constant through passage 5, most neurons in passage 1–3 were Tbr1- and Ctip2-positive. Satb2-positive neurons did not appear until passage 4. Data are mean \pm SEM. Scale bars = 50 μm . Abbreviation: DAPI, 4',6-diamidino-2-phenylindole.

but no Satb2-positive superficial layer neurons (data not shown). Satb2-labeled but Tbr1- and Ctip2-negative upper layer (layer II–IV) neurons started to appear and increase in number in the later passage RG (passages 4 and 5) (Fig. 3A, right). The passage-wise generation of subtypes of cortical neurons is quantified and summarized in Figure 3C. Although the total percentage of neurons stayed constant through passages 1–5, a switch was seen from around 80% deep layer neuron subtypes to 30%–40% superficial layer neurons as RG maturation progressed (Fig. 3C).

Late-Passage RG Generate Cortical Astrocytes and Interneurons

Cortical astrocytes are generated perinatally after the end of neurogenesis, and later stage RG are one of the main sources of cortical astrocytes [30]. After 150 days of culture with continuous passaging every 25 days, we observed an obvious change in cell morphology in the RG cultures. Although the early passage RG were process rich, with a mixture of dark cell bodies indicative of neurons and progenitors with long processes, the late passage RG had seemingly uniform cells with shorter and thicker processes. These cells continued to express nestin and vimentin, but BLBP expression was significantly reduced (Fig. 4A). The cells were proliferative (EdU labeled) and expressed Sox2+ (Fig. 4B), but they did not maintain processes during mitoses as did the early stage RG (Fig. 4C). In early RG culture, very few S100 β -positive cells were present compared with an abundance of S100 β astrocytes in the late cultures when cultured in serum containing medium. The rare early S100 β -positive cells were star-shaped and had long processes, and the late ones had a fibroblast-like astrocyte morphology with fewer and fatter processes (Fig. 4D). We also compared the culture composition between early and late passage RG culture. Both had around 13% total cells incorporating

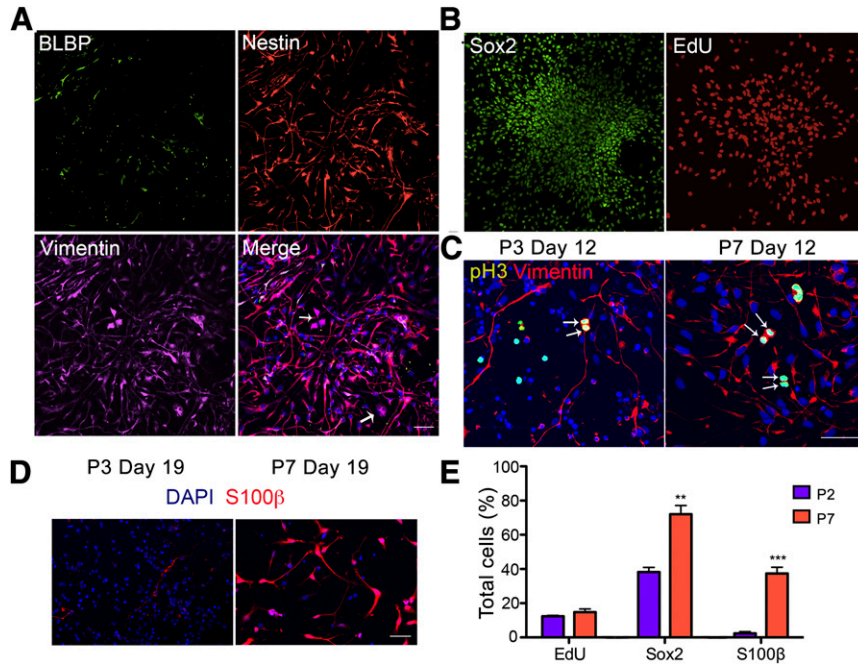


Figure 4. Transition of human embryonic stem cell-derived radial glia (RG) into a distinct late progenitor stage. **(A):** Late passage progenitors (P6 and beyond) lost expression of BLBP but retained nestin and vimentin expression. **(B):** Late passage progenitors are Sox2 positive and actively proliferating, as indicated by EdU labeling. **(C):** Early RG retained processes (left) during cell division, as indicated by pH3 staining but late progenitors did not (right). **(D):** The rare early passage (P3) S100β-positive astrocytes had stellate morphologies, and the abundant late (P7) ones were more fibroblast-like. **(E):** Quantification and comparison of marker expression among total cells in early (P2) and late (P7) passage RG cultures. The percentages of progenitors that incorporated EdU were similar between the two populations, and the late passage culture had significantly more Sox2- and S100β-positive cells. Data are mean \pm SEM. Student's *t* test, $n = 4$, **, $p < .001$; ***, $p < .0001$. Scale bars = 50 μ m. Abbreviations: BLBP, brain lipid-binding protein; DAPI, 4',6-diamidino-2-phenylindole; EdU, 5'-ethynyl-2'-deoxyuridine; P, passage; pH3, phosphorylated histone H3.

EdU, suggesting similar percentages of proliferating cells. However, the late cultures contained significantly more Sox2 ($72.0\% \pm 5.1\%$ compared with $38.3\% \pm 2.7\%$) and S100β ($37.3\% \pm 3.6\%$ compared with $2.3\% \pm 1\%$) positive cells ($n = 4$, Student's *t* test; Fig. 4E) compared with the early cultures. Thus, the early passage RG had transformed into a distinct late progenitor phenotype that has the capacity to generate astrocytes. To test the extent of astrocyte-generating capacity of these late progenitor cells, we treated them with either PBS or BMP4 (10 ng/ml) for 7 days and evaluated the resulting cell fates. The control group maintained progenitor properties as indicated by nestin staining with long-process bearing progenitor morphology but lacking GFAP staining with astrocyte morphology (Fig. 5A, top). The BMP4-treated cells had largely converted to intensively GFAP-labeled cells with typical astrocyte morphology (Fig. 5A, bottom). Both groups contained a small population of Tuj1-positive bipolar neurons that differed morphologically from the neurons in the early RG culture. Additional examination of these neurons revealed that they are positive for the interneuron marker GABA (Fig. 5B) but negative for the glutamatergic neuron marker Vglut1 (data not shown). These GABAergic neurons largely stained positive for calretinin (Fig. 5B, right), but not for parvalbumin or calbindin (data not shown). Quantification of cell type composition in late progenitor cultures showed $76.9\% \pm 3\%$ nestin-positive, GFAP-negative progenitors, $11.2\% \pm 2\%$ GFAP-positive cells, and $12\% \pm 1\%$ Tuj1-positive neurons. BMP4 treatment dramatically reduced nestin-positive progenitors to $2.1\% \pm 0.3\%$, pushing them toward GFAP-positive astrocytes at a percentage of $88\% \pm 0.7\%$, and the

Tuj1-positive neuronal population appeared to be unaltered in these 2 conditions (Fig. 5C). The differences between the late and early RG in differentiation (astrocyte vs. neuron; interneuron vs. cortical pyramidal neuron) combined with the differences at the progenitor level suggest that late passage RG culture represents a distinct population of progenitors that might correspond to SVZ progenitors *in vivo*. Markers that indicate dorsal-ventral identities such as Pax6, Emx1, and Mash1 are essentially absent at this late stage (data not shown).

hPSC-Derived RG Can Be Frozen at Specific Stages and Maintain Appropriate Progenitor and Progeny Subtypes

In the current methods for cortical neuron differentiation from hPSCs, cell culture is terminated after 90–120 days, and it is not possible to go back and retrieve intermediate stages. We therefore asked whether RG cryopreserved at different stages retain their stage-specific properties, thereby providing a readily accessible source for different cell types of interest. First, we found that, in addition to growing in culture as adherent monolayers, RG could also grow in suspension as neurospheres, allowing efficient expansion for studies that require large cell numbers (data not shown). Next, we froze RG using the normal splitting procedure and cryopreserved them in culture medium supplemented with 10% DMSO at different passages and characterized their phenotypes after thawing. We found that RG from both hESCs (Fig. 6) and hiPSCs (data not shown) could survive the freeze and thaw cycle at multiple passages. Moreover, early passage (passage 2 [P2]) RG

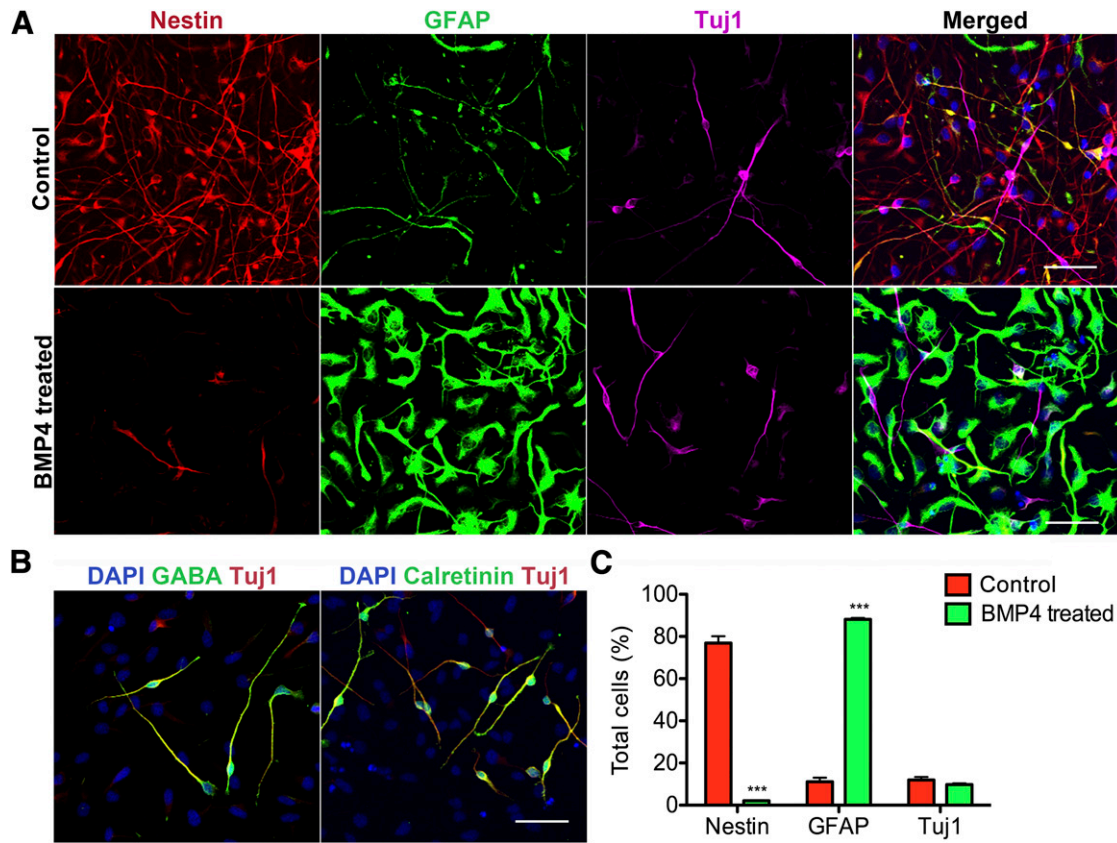


Figure 5. Late progenitors differentiate into highly pure populations of astrocytes on BMP4 treatment and are capable of generating interneurons. **(A):** Nestin-positive late progenitors with long processes largely transform into brightly GFAP-positive cells with typical astrocyte morphology with 7 days of 10 ng/ml BMP4 treatment. Tuj1-positive bipolar neurons are present in the culture before and after BMP4 treatment. **(B):** The bipolar Tuj1-positive neurons in late progenitor culture stain positive for GABA and calretinin. **(C):** Quantification of the cellular constituents of late progenitor cultures. Nestin-positive progenitors constitute $76.9\% \pm 3\%$ of the cells, and GFAP- and Tuj1-positive cells constitute $11.2\% \pm 2\%$ and $12\% \pm 1\%$, respectively. With BMP4 treatment (green bars), nestin-positive percentages significantly decreased to $2.1\% \pm 0.3\%$. GFAP-positive astrocytes constituted $88\% \pm 0.7\%$ of the entire culture and the Tuj1-positive neuronal population was not significantly altered ($9.8\% \pm 0.5\%$). Data are mean \pm SEM. Student's *t* test, $n = 6$, ***, $p < .0001$. Scale bars = $50 \mu\text{m}$. Abbreviations: BMP4, bone morphogenetic protein 4; DAPI, 4',6-diamidino-2-phenylindole; GFAP, glial fibrillary acidic protein.

maintained the potential to generate Tbr1-positive deep layer neurons but did not gain the competence to generate Satb2-positive superficial layer neurons after thawing (Fig. 6A). In contrast, P4 RG which had the competence to generate superficial layer neurons (Satb2+) maintained that potential after thawing (Fig. 6B). Late passage P7 RG were gliogenic both before and after thawing (Fig. 6C). Similar percentages of neuron subtypes and astrocytes before and after thawing were also observed in these characterizations.

hESC-Derived RG Engraft Into Embryonic VZ and Follows Developmental Cues to Migrate, Differentiate, and Integrate Properly

To further assess the developmental potential of the human RG, we performed in utero ventricular transplantation into mice to analyze the ability of the cells to migrate, differentiate, and integrate into the cortex. A GFP lentivirus was used to label passage 3 cells in culture, the cells were injected into the lateral ventricle region of embryonic day 14 mouse brains, and the mice were sacrificed on postnatal day 3. Many radially oriented GFP-positive pyramidal cells were found at different depths in the cortical plate, with a few tangentially

oriented cells present in the marginal zone (Fig. 7A). Green cells with an astrocyte morphology and positive GFAP staining were occasionally found at the pial surface among the host glial limitans and in the marginal zone (Fig. 7B). A number of bipolar GFP-expressing cells with a RG-like morphology localized to the lateral ventricle parallel to host vimentin-positive radial cells (Fig. 7C). Extensive GFP-positive radially oriented processes started near the lateral ventricle and extended to the cortex (Fig. 7D). Radial orientation was defined as the direction of neurites in the symmetrical 90° region perpendicular to the pial surface (Fig. 7E). Of all the GFP-labeled cells, $91.3\% \pm 3.4\%$ assumed a pyramidal neuronal morphology and $8.6\% \pm 3.4\%$ had astrocyte morphology (Fig. 7E). More than 90% of the neurons were radially oriented. GFP-positive neurons that migrated into the cortex localized to the correct cortical layer and expressed the layer-specific marker Ctip2 (Fig. 7F). Synaptophysin-stained host processes made contact with GFP-positive neuronal processes (Fig. 7G), suggesting that the neurons might have integrated functionally into the host cortex. In summary, grafted hESC-derived RG were able to localize to the lateral ventricle, orient properly, and differentiate into neurons and astrocytes that recognized migrational cues to end up at the appropriate final destination.

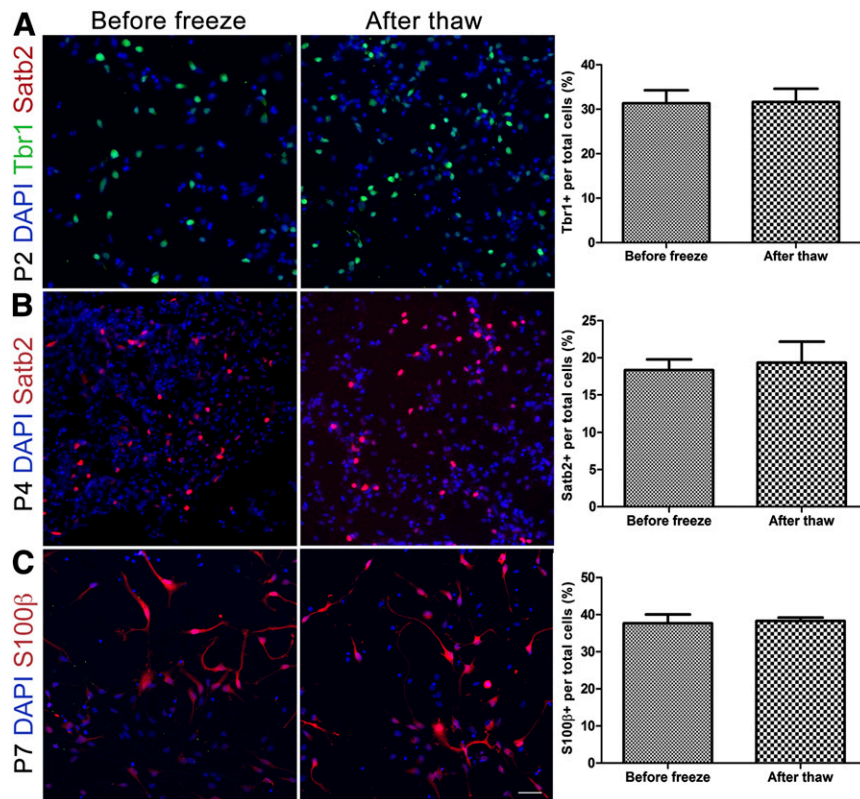


Figure 6. Human embryonic stem cell-derived radial glia (RG) survive freeze-thaw cycles and retain passage-appropriate characteristics. **(A):** Tbr1-expressing deep layer neurons rather than Satb2-positive neurons are present after thawing of P2 RG, the same as before freezing. **(B):** P4 radial glia preserved competence to generate Satb2-expressing superficial layer neurons after thawing. **(C):** P7 RG generate S100 β -positive astrocytes before and after thawing. Right: Bar graphs comparing percentage of relevant progenies within the culture at each passage. Abbreviations: DAPI, 4',6-diamidino-2-phenylindole; P, passage.

DISCUSSION

Evolution of the human cortex resulted in significant differences in the cell types, morphology, gene expression, and functions from mouse cortex. Because of the limited access to human tissue, isolation of human stem and progenitor cells and the lineages they produce is critical to our understanding of how the enormous diversity of cell types is produced in the human brain, to provide a model system to study central nervous system disease mechanisms, and to guide future attempts to harness stem cells for brain repair. In the present report, we describe an efficient method for the controlled generation of human RG from pluripotent stem cells in a defined chemical medium without added morphogens. RG identity was validated using the following approaches: (a) a thorough analysis of molecular markers of RG combined with a radial morphology; (b) validation of the temporally appropriate sequential generation of cortical neurons and astrocytes; and (c) *in vivo* transplantation studies showing appropriate localization of progenitors in the lateral ventricle, pyramidal neurons in the corresponding cortical layer, and astrocytes within the glia limitans.

We first showed the progressive differentiation of neuroepithelial cells into the RG and subsequently into Tbr2-positive secondary progenitors. RG were clearly delineated by their unique bipolar or unipolar morphology with one long process, and RG expression of the BLBP and GFAP molecular markers clearly distinguished these cells from neuroepithelial cells. Unlike mouse RG in

which GFAP expression is low, human RG express high levels of GFAP [31, 32]. Previous studies have reported similar spindle-shaped bipolar cells with some progenitor marker staining, but these cells generated GABAergic neurons rather than exclusively glutamatergic pyramidal neurons, raising concerns about the cortical RG identity of these cells [12, 33]. Radial-shaped progenitors were also observed in cortical neuron cultures; however, their abundance was low compared with that of other progenitor types; therefore, they were not isolated or thoroughly characterized [15–17]. hPSC-derived neural stem cells have been shown to expand for multiple passages and to keep generating both neurons and astrocytes [33, 34]; however, the regional identities of these neurons and astrocytes are unclear, because GABAergic neurons predominate in these cultures.

Astrocytes are heterogeneous with respect to morphology, marker expression, and function. Owing to the lack of molecular markers, regional astrocyte development and patterning are still not well understood [35]. Few reports have described the generation of region-specific astrocytes from hPSCs. Krencik et al. [36] reported that the patterning of neuroepithelial cells with fibroblast growth factor 8 (FGF8), followed by EGF/FGF2 expansion of progenitors, gives rise to presumptive cortical astrocytes after 180 days [36]. Although the timeline of cortical astrocyte generation matched our observation, it is unclear whether the Foxg1-positive forebrain identity is retained after FGF8 patterning. We have shown stable maintenance of the dorsal forebrain identity of RG in the absence of morphogens, with the sequential

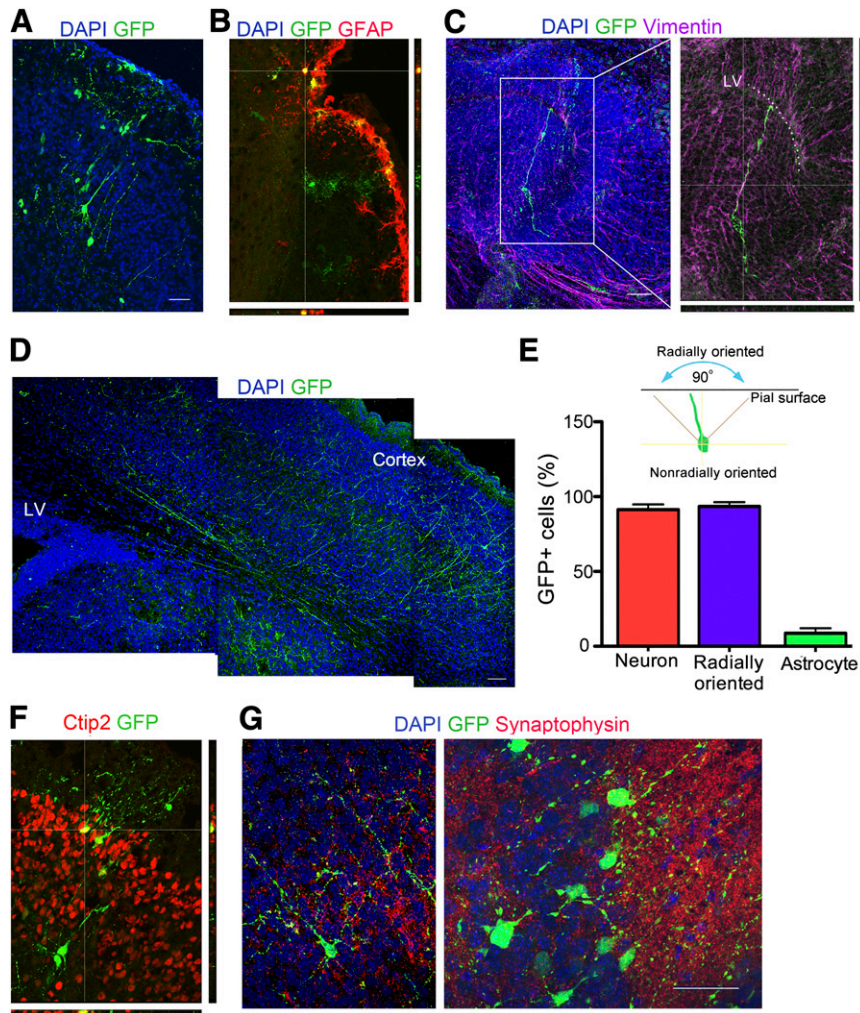


Figure 7. Differentiation, migration, and integration of engrafted GFP-labeled human embryonic stem cell-derived radial glia (RG) in mouse brain. E14 mouse brains were injected, and the brains were examined on postnatal day 3. **(A):** GFP-positive pyramidal neurons were radially arranged in the cortex. **(B):** GFP-positive cells with astrocyte morphology colocalize with GFAP in the outermost lining of the cortex. **(C):** Bipolar GFP-expressing cells with a RG-like morphology localize to the P3 LV, parallel to host vimentin-positive radial cells. Magnification, $\times 20$ (left), $\times 40$ (right). **(D):** Extensive GFP-positive radially oriented processes start near the LV and extend to the cortex. **(E):** Radial orientation is defined as the direction of neurites in the symmetrical 90° region perpendicular to the pial surface. Quantification of cells with neuronal or astrocytic morphology among the total GFP positive cells is shown. The percentage of radially oriented cells among the cells with neuronal morphology is also indicated. Data are mean \pm SEM, $n = 9$. **(F):** GFP-positive neurons localize to the correct cortical layer and express the layer-specific marker Ctip2. **(G):** Dotted synaptophysin stained host processes make contact with GFP-positive neuronal processes. Magnification, $\times 20$ (left), $\times 63$ (right). Scale bars = $50 \mu\text{m}$. Abbreviations: DAPI, 4',6-diamidino-2-phenylindole; GFAP, glial fibrillary acidic protein; GFP, green fluorescent protein; LV, lateral ventricle; P, passage.

specification of cortical neurons before the generation astrocytes, suggesting that these are cortical astrocytes. These findings also suggest radial glia follow an intrinsic mechanism to proceed through the subsequent lineages. Because it is an evolving, mixed culture, we hypothesized that signals from the differentiated lineages (e.g., cortical neurons) might promote the switch in the differentiation potential of progenitors at each stage. Exactly which signals govern radial glia lineage progression *in vivo* is also not known and will be more complex to tease out. Our *in vitro* paradigm might provide a platform to test this hypothesis in future experiments.

We also observed that astrocytic progeny were only found within the cortex after transplantation of the RG *in vivo*. Moreover, we found that RG differentiation into astrocytes went through a distinct late progenitor stage when BLBP expression

was lost and interneurons and astrocytes were produced. We also noted an interesting temporal difference in the morphology of S100 β -positive astrocytes. The rare early ones had long processes and the late ones assumed fibroblast-like morphology, with fewer and fatter processes (Fig. 4D). This is interesting, because in cortical astrocyte development, a sequential generation of protoplasmic astrocytes is found in the gray matter, followed by fibrous astrocytes populating the white matter. Although protoplasmic astrocytes contain few intermediate filaments, fibrous astrocytes will immunostain intensively for GFAP [33].

Cortical interneurons were traditionally thought to be exclusively ventral derived and composed of three main subtypes, based on the expression of parvalbumin, calretinin, or somatostatin, coming from different ventral regions [37]. However, recent studies have shown that dorsal RG also generate interneurons

postnatally in the mouse brain [38]. Furthermore, human dorsal RG have an even greater propensity to generate cortical interneurons that are GABA and calretinin positive [39], precisely matching what we observed in our late RG cultures. Our finding that hPSC-derived RG cultures give rise to a late progenitor type that generates cortical interneurons and astrocytes thus agrees with the findings *in vivo* and confirms the usefulness of this system to recapitulate key developmental events.

Human cortical progenitors were shown to have the remarkable ability to engraft and connect in the adult mouse brain [17]. Similarly, we found that hESC-derived RG followed developmental cues to differentiate and migrate to appropriate locations when injected into the E14 mouse lateral ventricle. This contrasts with previous transplantation of ES-derived neural precursors, which accessed large areas of both dorsal and ventral regions of the brain [40]. The developmentally appropriate behavior of our RG *in vivo* provides additional support for their identity and specificity.

We found that hPSC-derived RG can be maintained independent of aggregated rosette structures. Furthermore, they can be frozen at different stages and will retain their stage-specific properties after thawing. This is important, because it provides a practical method of accessing specific cortical neuronal or astrocytic stages without having to establish cultures *de novo*. The cell density was critically important for both the derivation and the maintenance of human RG from hPSCs. Low-density cultures did not generate RG from neuroepithelial cells, and the low density reduced the percentage of RG among the total cells in established RG cultures. High density was similarly noted to be important for the differentiation of pluripotent stem cells into neural progenitors and cortical neurons [26, 41]; however, the underlying mechanism is not known. RG express Notch-1, which is activated by ligands such as Delta-1 expressed by newborn neurons [3]. Disruption of Notch signaling inhibits the proper differentiation of RG, and activation of Notch promotes maintenance of the RG phenotype [27, 28]. It is thus not surprising that we found that Notch signaling exerted similar effects in our RG cultures.

CONCLUSION

We have successfully developed a protocol that generates developmentally accurate RG from human pluripotent stem cells. Such

RG cultures can be passaged and frozen and will demonstrate passage-wise sequential generation of the cortical neuron subtypes, cortical astrocytes and interneurons. In addition, we characterized a late progenitor stage that has the capacity to generate large numbers of cortical astrocytes and dorsal-derived cortical interneurons. Our findings are significant in terms of practically supplying a source of progenitors that can give rise to cortical pyramidal neurons, cortical astrocytes, or interneurons in a very short time frame compared with traditional methods. Furthermore, these cells display the appropriate sequential generation of neural cell types both *in vitro* and *in vivo*, suggesting they can be used to help define the mechanisms underlying the cell-intrinsic properties that lead to the generation of these different progeny.

ACKNOWLEDGMENTS

We thank Ljuba Lyass from the Stem Cell Core Facility of Northwestern University for help with cell culturing; Paul Mehl and Jeffery Nelson from the Flow Cytometry Core Facility of Northwestern University for help with fluorescence-activated cell sorting; and Hillary North and Su Ji Jeong from Northwestern University for suggestions and input with the experiments. This research is supported by NIH Grants R01NS20778, R01NS20013, and P30NS081774.

AUTHOR CONTRIBUTIONS

L.D.: conception and design, collection and assembly of data, data analysis and interpretation, manuscript writing; C.-Y.P.: data analysis and interpretation, manuscript editing; L.P.: collection of data; J.A.K.: financial support, administrative support, provision of study material, data analysis and interpretation, final approval of manuscript.

DISCLOSURE OF POTENTIAL CONFLICTS OF INTEREST

The authors indicated no potential conflicts of interest.

REFERENCES

- Götz M, Huttner WB. The cell biology of neurogenesis. *Nat Rev Mol Cell Biol* 2005;6:777–788.
- Anthony TE, Klein C, Fishell G et al. Radial glia serve as neuronal progenitors in all regions of the central nervous system. *Neuron* 2004;41:881–890.
- Malatesta P, Appolloni I, Calzolari F. Radial glia and neural stem cells. *Cell Tissue Res* 2008;331:165–178.
- Howard B, Chen Y, Zecevic N. Cortical progenitor cells in the developing human telencephalon. *Glia* 2006;53:57–66.
- Desai AR, McConnell SK. Progressive restriction in fate potential by neural progenitors during cerebral cortical development. *Development* 2000;127:2863–2872.
- Shen Q, Wang Y, Dimos JT et al. The timing of cortical neurogenesis is encoded within lineages of individual progenitor cells. *Nat Neurosci* 2006;9:743–751.
- LaMonica BE, Lui JH, Wang X et al. OSVZ progenitors in the human cortex: An updated perspective on neurodevelopmental disease. *Curr Opin Neurobiol* 2012;22:747–753.
- Bonfanti L, Peretto P. Radial glial origin of the adult neural stem cells in the subventricular zone. *Prog Neurobiol* 2007;83:24–36.
- Merkle FT, Tramontin AD, Garcia-Verdugo JM et al. Radial glia give rise to adult neural stem cells in the subventricular zone. *Proc Natl Acad Sci USA* 2004;101:17528–17532.
- LaMonica BE, Lui JH, Hansen DV et al. Mitotic spindle orientation predicts outer radial glial cell generation in human neocortex. *Nat Commun* 2013;4:1665.
- Wilson PG, Stice SS. Development and differentiation of neural rosettes derived from human embryonic stem cells. *Stem Cell Rev* 2006;2:67–77.
- Nat R, Nilbratt M, Narkilahti S et al. Neurogenic neuroepithelial and radial glial cells generated from six human embryonic stem cell lines in serum-free suspension and adherent cultures. *Glia* 2007;55:385–399.
- Liour SS, Yu RK. Differentiation of radial glia-like cells from embryonic stem cells. *Glia* 2003;42:109–117.
- Liour SS, Kraemer SA, Dinkins MB et al. Further characterization of embryonic stem cell-derived radial glial cells. *Glia* 2006;53:43–56.
- Shi Y, Kirwan P, Smith J et al. Human cerebral cortex development from pluripotent stem cells to functional excitatory synapses. *Nat Neurosci* 2012;15:477–486.
- Mariani J, Simonini MV, Palejev D et al. Modeling human cortical development *in vitro* using induced pluripotent stem cells. *Proc Natl Acad Sci USA* 2012;109:12770–12775.
- Espuny-Camacho I, Michelsen KA, Gall D et al. Pyramidal neurons derived from human pluripotent stem cells integrate efficiently into mouse brain circuits *in vivo*. *Neuron* 2013;77:440–456.
- Duan L, Bhattacharyya BJ, Belmadani A et al. Stem cell derived basal forebrain cholinergic

neurons from Alzheimer's disease patients are more susceptible to cell death. *Mol Neurodegener* 2014;9:3.

19 Watanabe K, Kamiya D, Nishiyama A et al. Directed differentiation of telencephalic precursors from embryonic stem cells. *Nat Neurosci* 2005;8:288–296.

20 Hevner RF, Neogi T, Englund C et al. Cajal-Retzius cells in the mouse: Transcription factors, neurotransmitters, and birthdays suggest a pallial origin. *Brain Res Dev Brain Res* 2003;141:39–53.

21 Haubst N, Berger J, Radjendirane V et al. Molecular dissection of Pax6 function: The specific roles of the paired domain and homeodomain in brain development. *Development* 2004;131:6131–6140.

22 Heins N, Malatesta P, Cecconi F et al. Glial cells generate neurons: The role of the transcription factor Pax6. *Nat Neurosci* 2002;5:308–315.

23 Ahlgren S, Vogt P, Bronner-Fraser M. Excess FoxG1 causes overgrowth of the neural tube. *J Neurobiol* 2003;57:337–349.

24 Miyoshi G, Fishell G. Dynamic FoxG1 expression coordinates the integration of multipolar pyramidal neuron precursors into the cortical plate. *Neuron* 2012;74:1045–1058.

25 Sessa A, Mao CA, Hadjantonakis AK et al. Tbr2 directs conversion of radial glia into basal precursors and guides neuronal amplification by indirect neurogenesis in the developing neocortex. *Neuron* 2008;60:56–69.

26 Shi Y, Kirwan P, Livesey FJ. Directed differentiation of human pluripotent stem cells to cerebral cortex neurons and neural networks. *Nat Protoc* 2012;7:1836–1846.

27 Gaiano N, Nye JS, Fishell G. Radial glial identity is promoted by Notch1 signaling in the murine forebrain. *Neuron* 2000;26:395–404.

28 Hatakeyama J, Bessho Y, Katoh K et al. Hes genes regulate size, shape and histogenesis of the nervous system by control of the timing of neural stem cell differentiation. *Development* 2004;131:5539–5550.

29 Patten BA, Sardi SP, Koirala S et al. Notch1 signaling regulates radial glia differentiation through multiple transcriptional mechanisms. *J Neurosci* 2006;26:3102–3108.

30 Molofsky AV, Krencik R, Ullian EM et al. Astrocytes and disease: A neurodevelopmental perspective. *Genes Dev* 2012;26:891–907.

31 Voigt T. Development of glial cells in the cerebral wall of ferrets: Direct tracing of their transformation from radial glia into astrocytes. *J Comp Neurol* 1989;289:74–88.

32 Cameron RS, Rakic P. Glial cell lineage in the cerebral cortex: A review and synthesis. *Glia* 1991;4:124–137.

33 Conti L, Pollard SM, Gorba T et al. Niche-independent symmetrical self-renewal of a mammalian tissue stem cell. *PLoS Biol* 2005;3:e283.

34 Falk A, Koch P, Kesavan J et al. Capture of neuroepithelial-like stem cells from pluripotent

stem cells provides a versatile system for in vitro production of human neurons. *PLoS One* 2012;7:e29597.

35 Hewett JA. Determinants of regional and local diversity within the astroglial lineage of the normal central nervous system. *J Neurochem* 2009;110:1717–1736.

36 Krencik R, Weick JP, Liu Y et al. Specification of transplantable astroglial subtypes from human pluripotent stem cells. *Nat Biotechnol* 2011;29:528–534.

37 Xu Q, Cobos I, De La Cruz E et al. Origins of cortical interneuron subtypes. *J Neurosci* 2004;24:2612–2622.

38 Ventura RE, Goldman JE. Dorsal radial glia generate olfactory bulb interneurons in the postnatal murine brain. *J Neurosci* 2007;27:4297–4302.

39 Yu X, Zecevic N. Dorsal radial glial cells have the potential to generate cortical interneurons in human but not in mouse brain. *J Neurosci* 2011;31:2413–2420.

40 Wernig M, Tucker KL, Gornik V et al. Tau EGFP embryonic stem cells: An efficient tool for neuronal lineage selection and transplantation. *J Neurosci Res* 2002;69:918–924.

41 Koch P, Opitz T, Steinbeck JA et al. A rosette-type, self-renewing human ES cell-derived neural stem cell with potential for in vitro instruction and synaptic integration. *Proc Natl Acad Sci USA* 2009;106:3225–3230.



See www.StemCellsTM.com for supporting information available online.